Emissivity Statistics in Turbulent, Compressible MHD Flows and the Density-Velocity Correlation

Alex Lazarian[1], Dmitri Pogosyan[2], Enrique Vázquez-Semadeni[3], and Bárbara Pichardo[4]
[1]Dept. of Astronomy, University of Wisconsin, Madison, USA
[2]Canadian Institute for Theoretical Astrophysics, University of Toronto, CANADA
[3]Instituto de Astronomía, UNAM, Campus Morelia, Apdo. Postal 3-72, Xangari, 58089, Morelia, Mich., MEXICO
[4]Instituto de Astronomía, UNAM, Apdo. Postal 70-264, México D.F. 04510, MEXICO

ABSTRACT

In this paper we test the results of a recent analytical study by Lazarian and Pogosyan, on the statistics of emissivity in velocity channel maps, in the case of realistic density and velocity fields obtained from numerical simulations of MHD turbulence in the interstellar medium (ISM). To compensate for the lack of well-developed inertial ranges in the simulations due to the limited resolution, we apply a procedure for modifying the spectral slopes of the fields while preserving the spatial structures. We find that the density and velocity are moderately correlated in space and prove that the analytical results by Lazarian and Pogosyan hold in the case when these fields obey the fluid conservation equations. Our results imply that the spectra of velocity and density can be safely recovered from the position-position-velocity (PPV) data cubes available through observations, and confirm that the relative contributions of the velocity and density fluctuations to those of the emissivity depend on the velocity resolution used and on the steepness of the density spectral index. Furthermore, this paper supports previous reports that an interpretation of the features in the PPV data cubes as simple density enhancements (i.e., "clouds") can be often erroneous, as we observe that changes in the velocity statistics substantially modify the statistics of emissivity within the velocity data cubes.

Subject headings: interstellar medium: general, structure-turbulence-radio lines; atomic hydrogen

1. Introduction

It is generally accepted that interstellar turbulence plays a crucial role in many astrophysical processes, including molecular cloud and star formation, mass and energy transfer in accretion disks, acceleration of cosmic rays, etc. At present we are still groping for the basic facts related to this complex phenomenon and one of the reasons for such an unsatisfactory state of affairs is that the interstellar turbulence statistics are not directly available. For instance, in studies of the neutral medium, indirect measures, such as spectral line widths and centroids of velocity, are employed (e.g. Miesch & Bally 1994; see also the review by Scalo 1987), while potentially more valuable sources of information available in velocity-channel maps remain mostly untapped (although see Heyer & Schloerb 1997; Rosolowsky et al. 1999; Brunt & Heyer 2000) because of the difficulty of relating the two-dimensional (2D) statistics available through observations to the underlying three-dimensional (3D) statistics. A discussion of various approaches to the problem of turbulence study using spectral line data can be found in a recent review by Lazarian (1999).

In particular, the problem has been recently addressed by Lazarian & Pogosyan (2000, herafter LP00), who derived the index (i.e., the logarithmic slope) of the power spectrum[1] of the intensity in velocity channel maps as a function of the corresponding indices for the 3D density and velocity fields of the emitting medium. Their work effectively provides a means of inverting the problem, so that the power spectra of the medium's density and velocity can be retrieved from the power spectrum of the emissivity. Note that this procedure involves considering channels of various velocity widths or "velocity slices of different thickness", in the terminology of LP00. Otherwise there is an indetermination due to the fact that for sufficiently shallow density spectra the emissivity in slices is given by a linear combination of the velocity and density indices. Recent measurements by Stanimirivic (2000) and Stanimirivic & Lazarian (2000) have confirmed a variation of the spectral index of HI intensity maps as the slice width is varied, in accordance with the predictions of LP00. The approach suggested by LP00 allows, in principle, to use the wealth of existing spectroscopic data for deriving interstellar turbulence statistics, thus possibly permitting new levels of understanding of this phenomenon. However, the derivation of LP00 assumes that the statistics of velocity and density are independent. Although those authors showed that for a particular case their results hold even when maximal correlation of velocity and density is assumed, testing the scheme on realistic fields from compressible magneto-hydrodynamic (MHD) simulations is essential.

In this paper we assess the degree of correlation between the density and velocity fields from MHD, compressible turbulence simulations, and whether the theoretical results from LP00 apply in this case, our goal being to find out to what extent the spectra of velocity and density can be recovered from the observed emissivity statistics. Note that if the interdependence of velocity and density is important for the recovery of their spectral indices, the inversion must be modified to account for the velocity-density correlations.

Numerous measurements of the emissivity within actual data cubes suggest that the spectrum follows a power law (Green 1993, Stanimirovic et al. 1999), as is the case in classical high-Reynolds number incompressible turbulence (e.g., Lesieur 1990), and high-resolution numerical simulations of highly compressible MHD turbulence in less than three dimensions (e.g., Passot, Vázquez-Semadeni & Pouquet 1995; Gammie & Ostriker 1996). A power-law assumption was also used by LP00. Numerical simulations of the ISM in 3D, however, usually do not have a large enough inertial range to produce good power laws and this can complicate our interpretation of the results. To deal with this issue, below we describe a procedure for "correcting" the spectral indices of the numerically-simulated density and velocity fields while preserving their underlying spatial correlations.

We describe the way how our numerical data were produced, and the correlation between density and line-of-sight velocity in section 2, compare numerical results with the predictions of LP00 in section 3, and provide a general discussion in section 4. Finally, our conclusions are summarized in section 5.

2. Numerical Data

[1]Note that throughout this paper we refer exclusively to the *spatial* power spectrum of the various fields, i.e., the Fourier transform of their auto-correlation function, as is common in turbulence studies. Such spectra should not be confused with, for example, spectral line profiles, or the spectra of time series of data, which we do not consider here. Also, throughout this paper, we stick to the convention that the spectral index of an N-dimensional field does *not* include the k^{N-1} factor corresponding to a summation over a shell of wavenumbers of radius k. With this notation, the well-known Kolmogorov $-5/3$ law corresponds to an index of $-11/3$.

2.1. Simulations and Spectrum Modification

In order to test whether the results from the analytical study of LP00 carry over to the case when the density and velocity fields are correlated according to self-consistent fluid evolution, in the following sections we explicitly calculate the spectral slopes for velocity channel-map data in position-position-velocity (PPV) cubes obtained from a three-dimensional simulation of the ISM at intermediate size scales (3–300 pc). The simulation is nearly identical to the one presented by Pichardo et al. (2000), except at slightly lower resolution. Both the simulation and the procedure for obtaining the velocity channel data have been discussed at length in that paper, and we refer the reader to it for details. In this section we just outline the information necessary for the purposes of the present paper. Channel maps are essentially maps of column density within a given line-of-sight (LOS) velocity interval. Throughout this paper we refer to such column density as "emissivity" or "map intensity", in analogy to the observational situation. For the sake of simplicity, thermal broadening, whose effects on the statistical analysis are discussed by LP00, is not considered.

The simulation represents a cubic box of 300 pc on a side on the Galactic plane, centered at the solar Galactocentric distance. The magneto-hydrodynamic equations are solved on a 100^3 Cartesian grid with the x, y and z directions respectively representing the radial, tangential and vertical directions in the Galactic disk. A pseudospectral scheme with periodic boundary conditions is used, which includes self-gravity, parameterized heating and cooling, and modeled star formation, such that a "star" (a local heating source which causes its surroundig gas to expand) is turned on wherever the density exceeds a threshold ρ_c and $\nabla \cdot \mathbf{u} < 0$. The "stars" remain on for 3.7 Myr after the criterion is met. This procedure is intended to mimic HII region expansion from OB star ionization heating, and provides an energy source for maintaining the turbulence in the simulation. Energy injection by supernovae is not included due to limitations of the numerical scheme, but the total energy injected per stellar event over the stellar lifetime is of the same order of magnitude as that which would be injected by a supernova event. The simulations also include the Coriolis force corresponding to a rotation of the frame around the Galactic center every 2×10^8 yr, and a shear in the x-y plane of the form $u_0 = 2.4 \sin(2\pi y/300 \text{ pc})$ km s^{-1}, where u is the x-component of the velocity field. The turbulent motions occur on top of this shearing velocity. This sinusoidal shear is not highly realistic, but is the only one possible with periodic boundary conditions, and was introduced by Passot et al. (1995) as a crude approximation of the galactic shear. Due to the periodic boundary conditions, no stratification is present in the z-direction, but this is not too strong a concern given the range of scales represented by the simulation.

Because the star formation prescription prevents the density from reaching values significantly larger than ρ_c, we turn it off after the turbulence is fully developed, and focus on a snapshot of the simulation shortly after that time. At the time of the snapshot, the maximum and minimum values of the (number) density are 109 and 0.43 cm^{-3}, respectively. A uniform magnetic field of 1.5 μG parallel to the x-direction is included, on top of which turbulent magnetic fluctuations induced by the stellar energy injection occur. The maximum and minimum values of the magnetic field strength are 12.5 and $4.5 \times 10^{-2} \mu$G. An image of the density field is shown in fig. 1a. We adopt the z-direction in the simulation (perpendicular to the Galactic plane) as the LOS direction, in order to prevent the shear from introducing power unrelated to the turbulent fluctuations into the velocity spectrum. Other than that, since the simulation has no vertical stratification, the z direction is statistically equivalent to the y direction. Only the x-direction, parallel to the mean magnetic field, is special. Figure 1b shows an image of the LOS-component of the velocity field. The structures in the simulations have been discussed at length by Pichardo et al. (2000).

However, neither the density nor the LOS-velocity fields have spectra well suited for studying the emissivity spectrum since, due to the low resolution of the simulation, the spectra are not clear power laws, while most turbulence theories, including LP00's, consider power-law spectra. To circumvent this problem, in what follows we use modified density and velocity fields, such that their spectra are indeed power laws, but the phase coherence of the original fields is preserved. A partial justification for this procedure stems from the fact that the spatial information is contained in the phases of the Fourier decomposition of a given field, while the spectrum is related exclusively to the relative amplitudes of the various modes (Armi & Flament 1985). Unfortunately, this justification is not complete, because the velocity-density coherence does change to some extent as the spectral slope is modified. We discuss this issue in some more detail in §2.2.

As an indication of what would be realistic indices for the fields, we note that incompressible MHD simulations that resolve the inertial range (Cho & Vishniac 2000a,b) tend to result in a Kolmogorov-type spectrum with slope $-11/3$, as theoretically predicted by Goldreich & Shridhar (1995), while highly compressible simulations in less than 3D (e.g., Passot et al. 1995; Scalo et al. 1998 [2D]; Gammie & Ostriker 1996 [1+2/3 D]) tend to give shock-spectra for the velocity with slopes near -4 and density spectra with slopes near -2. Thus, one may expect spectral indices close to these values also in 3D highly compressible turbulence, so that the spatial correlations from our simulations should probably be most appropriate for those ranges of values. On the other hand, we do not know beforehand what sort of phase coherence should be present for either shallower or steeper spectra, and therefore in these cases our present study is limited to testing whether the formulae by LP00 are correct in the presence of the particular sort of correlations produced by our simulations.

The spectral index modification procedure is as follows. We perform a Fourier decomposition of the density and LOS velocity as

$$\rho(\mathbf{x}) = \sum_{\mathbf{k}} \rho_{\mathbf{k}} \exp\left(i\mathbf{k}\cdot\mathbf{x}\right) \tag{1}$$

$$u_z(\mathbf{x}) = \sum_{\mathbf{k}} u_{\mathbf{k}} \exp\left(i\mathbf{k}\cdot\mathbf{x}\right), \tag{2}$$

where $\mathbf{x}$ is the position vector, $\rho_{\mathbf{k}}$ and $u_{\mathbf{k}}$ are the Fourier amplitudes of the fields (we drop the subindex z in the latter for convenience) and $\mathbf{k}$ is the (vector) wavenumber. In general, the amplitudes are of the form $X_{\mathbf{k}} = |X_{\mathbf{k}}|e^{i\phi}$, where $|X_{\mathbf{k}}|$ and ϕ are respectively the magnitude and phase of $X_{\mathbf{k}}$. Thus, we replace the magnitudes of both fields by new ones (labeled by primes) satisfying $|X_{\mathbf{k}}{}'|^2 \propto k^n$, where n is the desired power-law index. The phases are unchanged. The modified amplitudes are then transformed back to configuration space, rendering new fields which preserve the spatial structure of the original fields but with the desired power-law spectrum. We avoid aliasing by including only modes with wavenumbers lying within a circle of radius equal to half the resolution in wavenumber space in the inverse transform. As an example, in fig. 2 we show the original power spectrum of the density field together with the resulting modified spectrum for $n = -4$, while fig. 3 shows cuts through the original and modified density fields, to appreciate the kind of structural changes arising from the spectrum-modification procedure. In the remainder of this paper, we reserve the symbol n for the index of the density power spectrum, and denote the velocity power (or energy) spectrum index by μ.

Using this procedure, we construct a suite of density fields with spectral indices -2.5, -4, and -5, and of velocity fields with spectral indices -3.2, -3.7 (the Kolmogorov value), and -4.5. From these, we then construct the corresponding PPV cubes for each density-velocity pair, which are used in the next section to obtain the projected intensity and velocity-channel maps.

2.2. Density-Velocity correlation

To characterize the correlation between velocity and density one can use the following function

$$C(\mathbf{r}) = \frac{\langle \rho(\mathbf{x})\ \mathbf{u}(\mathbf{x}+\mathbf{r}) \cdot \mathbf{r}/|r| \rangle}{\sigma_\rho \sigma_{\mathbf{u}}}, \tag{3}$$

where $\mathbf{r}$ is the spatial separation (or "lag"), $\mathbf{x}$ is the spatial position, ρ is the density field, $\mathbf{u}$ is the total three-dimensional velocity vector, and σ_ρ and $\sigma_{\mathbf{u}}$ are respectively the standard deviations of the density and of the velocity. The averaging is performed over all $\mathbf{x}$-space and over all angles of the lag vector $\mathbf{r}$. This function is similar to the function $F(\mathbf{r})$ introduced in LP00 to calculate the effect of maximal allowable velocity-density correlations. The difference between eq. (3) and $F(\mathbf{r})$ amounts to the normalization and the $\cos\theta$ dependence, where θ is the angle between $\mathbf{r}$ and the z-axis.

However, since the projection along $\mathbf{r}$ precludes computing this correlation using Fourier transform techniques, and computing the full correlation numerically in physical space would take prohibitely long times, in this paper we compute a related correlation involving only the LOS components of both the lags and of the velocity vector. This correlation, given by

$$C(|z|) = \frac{\langle \rho(\mathbf{x})\ \mathbf{u}(\mathbf{x}+\mathbf{z}) \cdot \mathbf{z}/|z| \rangle}{\sigma_\rho \sigma_{u_z}}, \tag{4}$$

is much more economical numerically, but contains the same essential information as eq. (3). In eq. (4), $\mathbf{z} = (0, 0, z)$ is the separation along the LOS and the averaging is performed over all positions $\mathbf{x}$ in the simulation box and over separations z and $-z$. This correlation is shown in fig. 4a for the original density and LOS-velocity fields.

As mentioned in §2.1, the correlations do change to some extent upon the change in spectral indices. We have observed that the correlation increases as the slopes of either the density or the velocity spectra are made steeper. Since a steeper (resp. shallower) slope means that the small scales are depressed (resp. enhanced) with respect to the large scales, the observation implies that the density and velocity fields are more similar to each other at large scales than at small ones. The correlation between the modified fields most resembles that between the original fields when the modified slopes are closest to those of the original spectra.

The correlations observed are moderate, having a maximum ~ 0.25 (in absolute value) for the original fields, and ~ 0.4 for the modified fields with steepest slopes. In retrospect, this result can be understood in terms of the fact that the fluid equations link one field with the spatial derivatives of the other: in the continuity equation, the density evolution is determined by the *divergence* of the velocity field, and in the momentum equation, the velocity evolution is linked to the pressure *gradient*, which at best can be related to the density gradient, if the flow behaves in an approximately barotropic way (e.g., Vázquez-Semadeni, Passot & Pouquet 1996). Thus, stronger correlations may be expected between the density and the velocity divergence, and between the velocity and the density gradient, but not so much between the plain density and LOS-velocity fields. Indeed, fig. 4b shows the correlation between the original density field and the divergence of the original 3D velocity field. A larger (negative) correlation, of up to -0.53 is seen, supporting this interpretation.

Whether or not a density-velocity correlation of the observed strength can alter the results of LP00 is not clear *a priori*, and this is the motivation for our study below.

3. Statistics of Velocity-Channel Maps

Unlike the observational situation, in numerical simulations the density and velocity fields are available directly. This allows us to simulate observations and to control the accuracy with which the individual 3D statistics are recovered.

Spectroscopic observations usually deal with velocity channel maps in which the velocity resolution is determined by the instrument. In the case of our numerical simulation, velocity resolution is not an issue, and we can produce as many velocity channels as desired from the original density and LOS-velocity data cubes. Surely the statistics within an individual slice are degraded as the slice gets thinner, producing progressively higher levels of shot noise, but we compensate for this effect by averaging over the whole set of slices available.

To compare our results with the theoretical predictions of LP00 we recall that two possible regimes were found there, depending on the width of the velocity channels. They were termed "thin" and "thick" slicings, and their emergence is well motivated physically. If we consider turbulence at a scale l, the expected squared velocity difference (the second-order structure function) between points separated a distance l scales as Cl^m , where m is 2/3 for Kolmogorov-type turbulence, and C is a constant that depends on the intensity of turbulence (see, e.g., Lesieur 1990). The structure function index m is related to the velocity power spectrum's index μ by $m = -\mu - 3$. Thus, when this velocity difference is larger than the width of the velocity slice, the slice is considered *thin*, and *thick* otherwise. LP00 showed that different slopes for the emissivity spectrum are expected in the two regimes mentioned above. It is obvious that whether the slice is either thick or thin with respect to the characteristic turbulent velocity difference depends on the scale being considered, and therefore, since the thin and thick asymptotics differ in general, we expect to see a change of the slope of the emissivity spectrum at some transition scale which depends on the channel width.

To test the predictions of LP00, in fig. 5 we plot the spectra of the emissivity fluctuations in velocity slices of the PPV data cubes ("channel maps") (*dash-dotted lines*), the spectra of the 3D density fields (*solid lines*), and the spectra of the density in thin spatial slices of the 3D density field (*dashed lines*), for various combinations of the density and velocity spectral slopes. These plots confirm the theoretical expectations. First of all, the transition from thick to thin slices depends on the spectral index of the velocity. For relatively small numbers of slices we have observed that the slices are still thin for shallow indices and show signatures of becoming effectively thicker for steep indices. The width of the slice is given by $\Delta V/N$, where $\Delta V = V_{\rm max} - V_{\rm min}$ and N is the number of slices. The value of ΔV along the LOS will be a factor of a few higher than the dispersion σ along the same LOS. Conservatively, we shall assume this factor to be 5, which corresponds to 2.5σ positive and negative excursions. The squared dispersion over the box size L, σ^2, equals CL^m for power-law statistics. Therefore, in order for the slice to be thin, it is required that $Cr^m > (2.5)^2 CL^m/N^2$, where r is the scale under consideration in the plane of the slice, and is essentially the inverse of wavenumber in the emissivity spectrum. This means that $N > 2.5(L/r)^{m/2}$. Another expected feature is the flattening of the spectrum at large k (small separations r) due to shot noise. In our case we derive the slope considering scales from $r \approx L$ down to $r \approx 0.1L$, where L is the length of the integration box. Figure 5 shows that for r smaller than $0.1L$ the emissivity spectrum indeed flattens.

The considerations above mean that for the steepest velocity index of -4.5 (i.e. $m = 1.5$), the number of slices should be larger than 30 in order for them to be thin. On the other hand, an increase in the number of slices results in higher shot noise due to the discrete sampling of the velocity along the line of sight (we only have 100 samples along each line of sight). Thus, we have adopted a slice width of $0.03\Delta V$, which we have found to correspond to thin slicing for the entire parameter space that we explore, but does

not introduce too high a level of shot noise.

For thin slices and sufficiently *steep* density spectra ($n < -3$), LP00 predicted that the measured emissivity spectrum *does not* depend on the density spectral slope, and has an index

$$(\textit{thin slice index if density spectrum is steep}) = -3 + m/2. \quad (5)$$

For example, for Kolmogorov turbulence, $m = 2/3$, and therefore an emissivity index of -2.66 is expected. Conversely, for *shallow* density spectra, i.e. when $n > -3$, the spectral index in thin slices is expected to be (LP00)

$$(\textit{thin slice index if density spectrum is shallow}) = n + m/2. \quad (6)$$

Table 1 provides a quantitative comparison between the theoretical predictions of LP00 and our numerical results, showing the spectral indices of the emissivity in the velocity channels as a function of the indices of the underlying density and velocity fields. The theoretical predictions of LP00 (given by equations (5) and (6)) are indicated in parentheses, while the measured values in the simulated fields are shown in bold type. It is seen that in all cases the agreement is within 10%, for both "shallow" and "steep" density spectral indices. We stress that the spectra of the 3D density and velocity data cubes, and of the 2D velocity slices, are obtained by integrating with the appropriate configuration space factors, which are r^2dr and rdr respectively.

The main prediction of LP00 is the importance of the velocity statistics in the determination of the emissivity statistics, specifically, its power spectrum. Our numerical results confirm this conclusion. Indeed, Table 1 shows that as the velocity spectral index is varied (downwards along the columns in Table 1), significant variations occur in the emissivity spectral index. Moreover, for steep density spectra, the emissivity statistics are roughly independent of the density spectral index. For example, consider the cases with velocity indices -3.2 and $-11/3$. It is seen that as the underlying density spectral index is changed from -4 to -5, the emissivity spectral index in thin channels remains constant within the precision of our measurements. For the case with velocity index of -4.5, the emissivity index changes slightly (from -2.1 to -2.3) for the same variation of the density index as above, but such slight change is within the uncertainty of 0.2, and brackets the value predicted by the LP00 theory. *By itself, this result sends a message of warning against attempts to interpret features in the velocity channel maps as actual density enhancements.*

The above discussion suggests that, whatever the velocity spectrum, it can be restored from observations. A possible ambiguity that arises in the case of shallow density spectra, when both the velocity and density contribute to the channel map spectrum, can be resolved by considering several slice widths. For example, it is obvious that if integration is performed over the whole velocity range, the resulting statistics can depend on the density only. The corresponding density inversion is discussed by Lazarian (1995). For power-law statistics, the spectral index for *very thick* velocity-integrated slices equals the spectral index of the underlying 3D density. We have verified this result by integrating over the velocity (the plots corresponding to the integrated 2D statistics coincide with those of the 3D spectra in fig. 5).

We have also confirmed other predictions from LP00, such as the change of the density spectral index from n in volume to $n + 1$ in a thin *spatial* density slice, as shown in fig. 5 by the dashed lines. Another important prediction of LP00 was the gradual steepening of the emissivity spectrum in the velocity slices as their width increases. This prediction was confirmed by Stanimirovic (2000) and Stanimirivic & Lazarian (2000) on the basis of 21 cm Small Magellanic Cloud data and fig. 6 shows that this indeed happens in our simulation data. In particular, the maximum possible thickening occurs when the velocity information is averaged out. In our case this corresponds to integration through the velocity box, or, equivalently, from an

Density index →	−2.5 (shallow)	−4 (steep)	−5 (steep)
Velocity index ↓			
−3.2	**−2.2** (−2.40)	**−2.9** (−2.90)	**−2.9** (−2.90)
−11/3	**−1.9** (−2.17)	**−2.6** (−2.67)	**−2.6** (−2.67)
−4.5	**−1.8** (−1.75)	**−2.1** (−2.25)	**−2.3**(−2.25)

Table 1: Spectral index of the emissivity fluctuations in *thin* velocity channels as a function of the density (top row) and velocity (left column) fields' spectral indices. The actual measured values are given in bold font, while the theoretical predictions are given in parentheses. The differences between the theoretical and observed values are within the uncertainties of determining the spectral slope. The uncertainty of the slope fittings is ~ 0.2, due to the effects of shot noise and slight imperfections in the spectrum modification procedure, $\sim \pm 0.1$ in the imposed spectral index.

integration throughout the full line of sight in the original 3D density data. It is evident that in this case the velocity fluctuations should not matter and only density statistics should influence the results. We have verified that both a pure density integration along the LOS and a velocity integration of the emissivity data cubes give the same spectral index.

4. Discussion

In §2.2 we have shown that the density and LOS-velocity fields in our ISM simulation are moderately correlated. An important question is whether there are interstellar situations in which the velocity-density correlations are much stronger than in our simulations and whether the results by LP00 are applicable to those situations. The answer to this question may be obtained by analyzing simulations of regions with physical conditions different from those assumed here. However, even in the case of strong correlations, the analytical results of LP00 may hold, as it was shown by LP00 for a particular case of maximal possible velocity-density correlations. Further research should clarify the issue.

Astrophysical implications of the asymptotic relations obtained in LP00 are discussed at length in Lazarian (1999). Here we will stress two points. First, the agreement between our measured emissivity spectral indices and the predictions of LP00 makes us more optimistic about the application of the LP00 technique to emission-line studies of actual interstellar turbulence. Second, it also gives us confidence that the interpretation by LP00 of the HI intensity spectrum (Green 1993; Stanimirovic et al. 1999) as arising from velocity fluctuations with a Kolmogorov (i.e., $-11/3$ spectral index) spectrum is correct.

It is worth pointing out that, even though the notion of Kolmogorov turbulence has been mentioned frequently throughout the paper, we do not wish to imply that the ISM in general exhibits Kolmogorov

turbulence. Arguments why the Kolmogorov (1941) description is not likely to be adequate for the ISM have been given by several authors (e.g., Scalo 1987; Passot, Pouquet & Woodward 1988; Lazarian 1995; Vázquez-Semadeni 1999; Vázquez-Semadeni et al. 2000). Briefly speaking, the ISM flow, unlike that in the Kolmogorov description, is magnetized and compressible. One would think that this should change the scaling. Indeed, strong compressibility may give rise to a spectrum of shocks, with a slope of -4 (in the notation convention used in this paper). On the other hand, a theory of magnetized, incompressible turbulence recently put forward by Goldreich and Sridhar (1995) predicts the same $k^{-11/3}$ Kolmogorov scaling for motions perpendicular to magnetic field lines. Such motions would dominate small-scale asymptotics and therefore the measured spectrum may stay Kolmogorov-like, although the nature of the cascade is influenced by magnetic field. Moreover, the interpretation of the observational data given in LP00, and supported in this paper, is suggestive that the Kolmogorov scaling may ultimately survive compressibility or, alternatively, that the HI data considered there sample gas that is only weakly compressible. Further work, both theoretical and observational, is needed to resolve this issue. In particular, application of the techniques used here to molecular-line data should prove of great interest.

To conclude we should stress that for Kolmogorov turbulence there exists a *coincidence* between the spectral index of a thin, 2D spatial slice of the density, which is:

$$(\textit{spectral index of thin 2D density slice}) = n + 1 \tag{7}$$

and the spectral index of the emissivity fluctuations in a thin velocity channel when the density spectrum is steep (e.g. Kolmogorov) and the velocity spectrum follows a Kolmogorov law. Indeed, the former, calculated using eq. (7), is $-11/3 + 1 = -8/3$ while the latter, calculated using eq. (5), takes the same value $-3 + 1/3 = -8/3$. Although the accidental character of this coincidence was mentioned in LP00, our experience shows that it does cause confusion. For instance, we have had to confront the point of view that the observed spectrum of HI fluctuations is a simple consequence of eq. (7). This is a *fallacy* and, while we do not wish to repeat the arguments of LP00, Table 1 shows that the naive "rule" given by eq. (7) does not return the correct emissivity spectral indices for velocity spectra other than Kolmogorov's, and that the coincidence is accidental for the Kolmogorov index. The correct formula for calculating the spectral index of the emissivity fluctuations in thin slices when the density spectrum is steep is given by eq. (5).

5. Summary and implications

In this paper we have used data from a numerical simulation of compressible MHD turbulence in the ISM to study the correlation between the density and LOS-velocity field, and the dependence of the spectral index of the velocity-channel emissivity on the indices of the original three-dimensional velocity and density fields. To do so, we have *a)* computed the cross-correlation between the density and LOS-velocity fields, *b)* modified their spectral slopes to pre-determined values, and *c)* produced PPV data from them.

From the PPV data, we computed in turn the emissivity spectrum in velocity slices of those cubes ("channel maps"), allowing us to directly test the results from the analytical study by LP00. We have found that its predictions hold also for the case of fields obeying the fluid conservation equations. In particular, we have found that for steep density spectra with power-law indices $n < -3$, the emissivity spectral index does not depend on the actual value of the density index and is determined exclusively by the velocity fluctuations. This indicates that only the velocity field is responsible for the structure existing in thin slices of the PPV cubes if the density spectrum is steep enough, in agreement with the previous result by Pichardo et al. (2000) that the morphology in the channel maps is more resemblant of that of the

LOS-velocity field than that of the density field, and with previous suggestions that "objects" identified in position-velocity maps may not correspond to actual density features (Adler & Roberts 1992; Pichardo et al. 2000; Ostriker, Stone & Gammie 2000).

The spectral index measured for the emissivity fluctuations in the numerical simulation was within 10% of the value given by relation (5), derived by LP00, in which m is the exponent of the second-order structure function. For a shallow density spectrum, namely $n > -3$, we found that the emissivity index depends on both velocity and density. Again the LP00 expression for the resulting power-law index, relation (6), provides a satisfactory description of our measurements. We also estimated the accuracy of our measurements both by integrating out the velocity within PPV data cubes and by taking thin slices of the density data cubes. These cases have straightforward analytical solutions (see LP00) and served as benchmarks. We also verified that variations of the emissivity spectrum resulting from the change of the velocity slice width (see fig. 6) are very similar to those reported in the studies by Stanimirovic (2000) and Stanimirovic & Lazarian (2000), in which the width of observational HI data slices was varied to test the predictions from LP00.

In brief, our results imply that:
1. Velocity creates small scale structure within slices of PPV data cubes and therefore the interpretation of features seen in PPV data cubes as density structures ("clouds") may be misleading.
2. For sufficiently shallow density spectra, velocity dominates the statistics of intensity fluctuations within PPV slices.
3. Emissivity spectra become steeper as the width of the velocity slices increases and, for sufficiently thick slices, the spectra are dominated by density enhancements only.

Part of this work was completed while two of us (A.L. and E.V.-S.) participated in the Astrophysical Turbulence Program of the Institute for Theoretical Physics at the University of California at Santa Barbara. The numerical simulation was performed on the Cray Y-MP 4/64 of DGSCA, UNAM. This work has received partial funding from CONACYT, México, through grant 27752-E to E.V.-S. and from NSF, USA, through grant PHY94-07194.

REFERENCES

Adler, D. D., & Roberts, W. W. 1992, ApJ, 384, 95

Armi, L. & Flament, P. 1985, J. Geophys. Research, 90, no. C6, 11779

Brunt, C. & Heyer, M. H. 2000, preprint (astro-ph/0011200)

Cho & Vishniac 2000a, ApJ, 539, 253

Cho & Vishniac 2000b, ApJ, 538, 217

Gammie, C.F. and Ostriker, E.C. 1996, ApJ 466, 814

Green, D.A. 1993 MNRAS, 262, 328

Goldreich, P. & Sridhar, S. 1995, ApJ, 438, 763

Kolmogorov, A. 1941, Compt. Rend. Acad. Sci. USSR, 30, 301

Heyer, M. H. & Schloerb. F.P 1997, APJ, 475, 173

Lazarian, A. 1995, A&A, 293, 507

Lazarian, A. 1999, in Plasma Turbulence and Energetic Particles, ed. M. Ostrowski and R. Schlickeiser, Cracow, 28, astro-ph/0001001

Lazarian & Pogosyan 2000, ApJ, 537, 720

Lesieur, M. 1990, Turbulence in Fluids, 2nd ed. (Dordrecht: Kluwer)

Miesch, M.S., & Bally, J. 1994, ApJ, 429, 645

Ostriker, E.C., Stone, J.M. & Gammie, C.F. 2000 (preprint: astro-ph/0008454)

Passot, T., Pouquet, A. & Woodward, P. 1988, A&A

Passot, T., Vázquez-Semadeni, E., & Pouquet, A. 1995

Pichardo, B., Vázquez-Semadeni, E., Gazol, A., Passot, T. & Ballesteros-Paredes, J. 2000, ApJ, 532, 353

Rosolowsky E.W., Goodman, A.A., Wilner, D.J., & Williams, J.P. 1999, ApJ, 524, 887

Scalo, J.M. 1987, in Interstellar Processes, eds. D.F. Hollenbach & H.A. Thronson, Reidel, Dordreicht, 349

Scalo, J.M., Vázquez-Semadeni, E., Chappell, D. & Passot, T. 1998, ApJ, 504, 835

Stanimirovic, S. 2000, in "The Evolution of Galaxies: Observational Clues", eds. J.M. Vilchez, G. Stasinska & E. Perez (in press)

Stanimirovic, S. & Lazarian, A. 2000, ApJ, submitted

Stanimirovic, S., Staveley-Smith, L., Dickey, J.M., Sault, R.J., & Snowden, S.L. 1999, MNRAS, 302, 417

Vázquez-Semadeni, E., Passot, T. & Pouquet, A. 1996, ApJ, 473, 881

Vázquez-Semadeni, E. 1999, in Millimeter & Submillimeter Astronomy: Chemistry and Physics in Molecular Clouds", eds. W. F. Wall, A. Carramiñana, L. Carrasco, and P. F. Goldsmith (Dordrecht: Kluwer), 161

Vázquez-Semadeni, E., Ostriker, E. C., Passot, T., Gammie, C. & Stone, J. 2000, in "Protostars & Planets IV", eds. V. Mannings, A. Boss & S. Russell (Tucson: Univ. of Arizona Press), 3

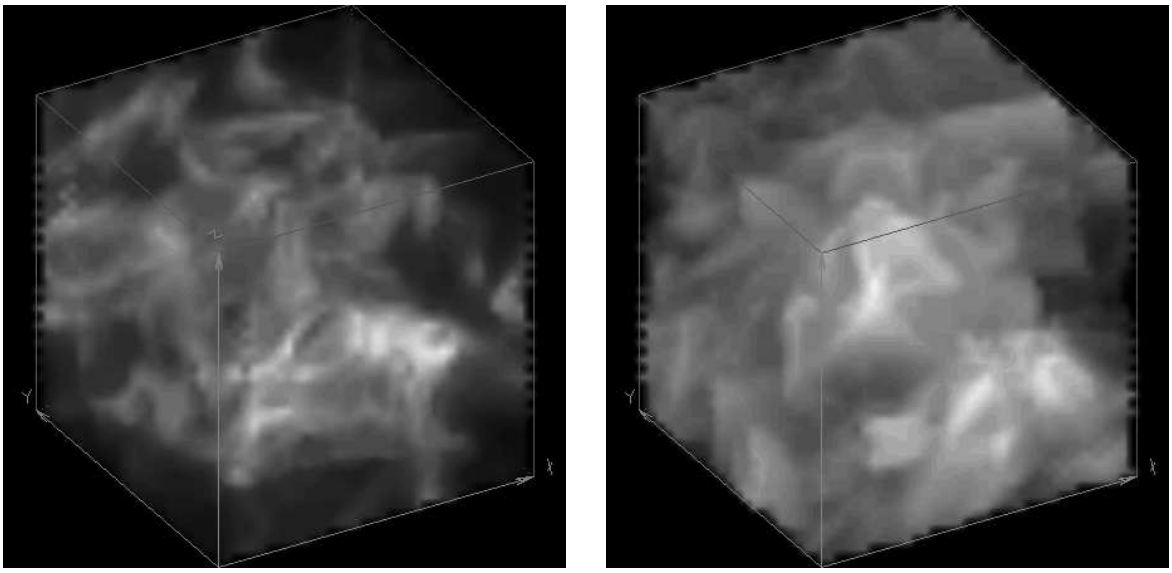

Fig. 1.— *a) (Left Panel)* Three-dimensional (3D) logarithmic image of the original density field. The maximum and minimum density values are 109 and 0.43 cm^{-3}. *b) (Right panel)* 3D image of the LOS-velocity field, i.e., the z-component of the velocity vector. In both cases, whiter color means larger values.

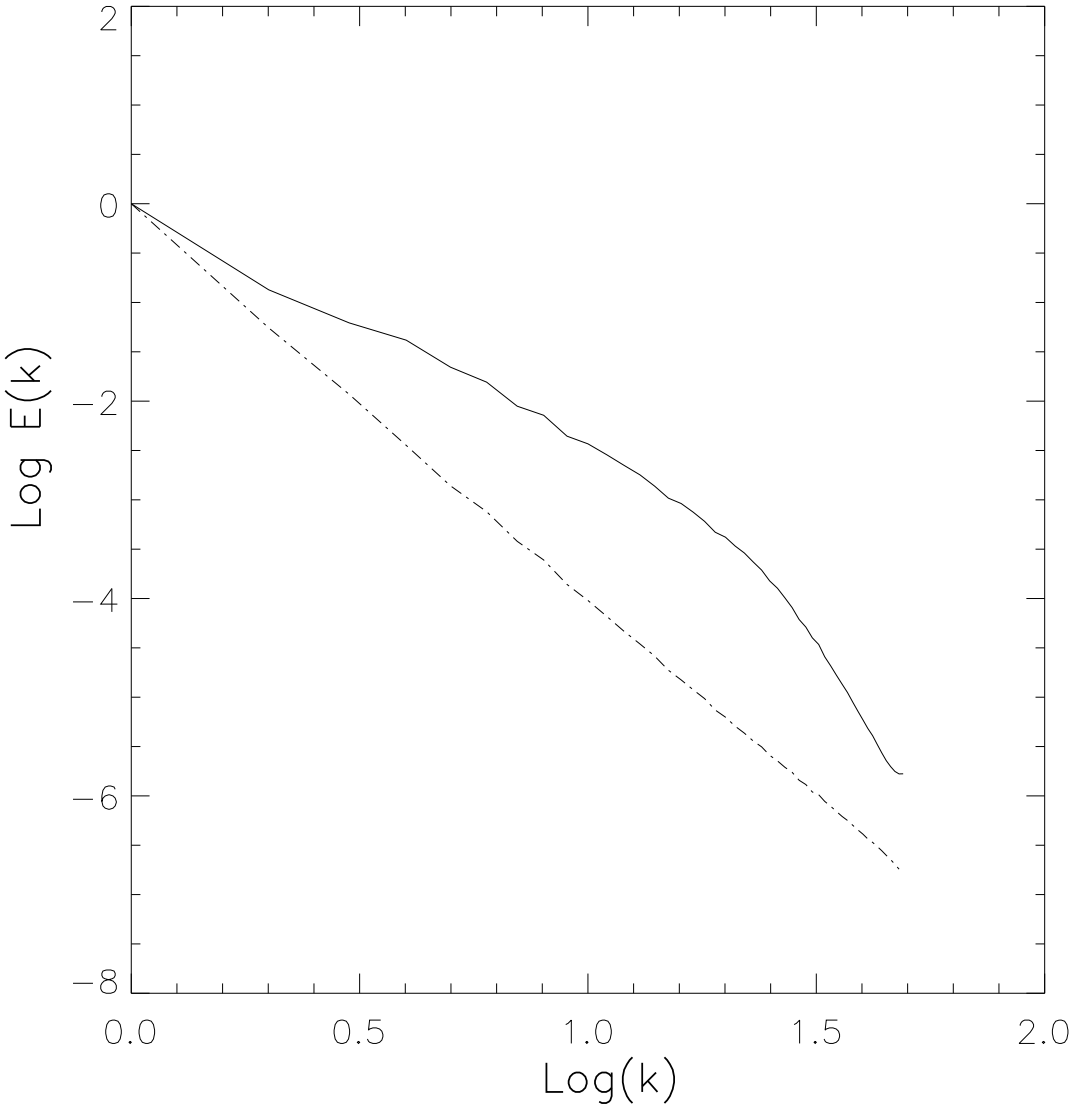

Fig. 2.— Spectra of the density field in original form (*solid line*) and after modification to an index of −4 (*dash-dotted line*). The wavenumber k here is defined as L/λ, where λ is the wavelength associated with k, and L is the box size.

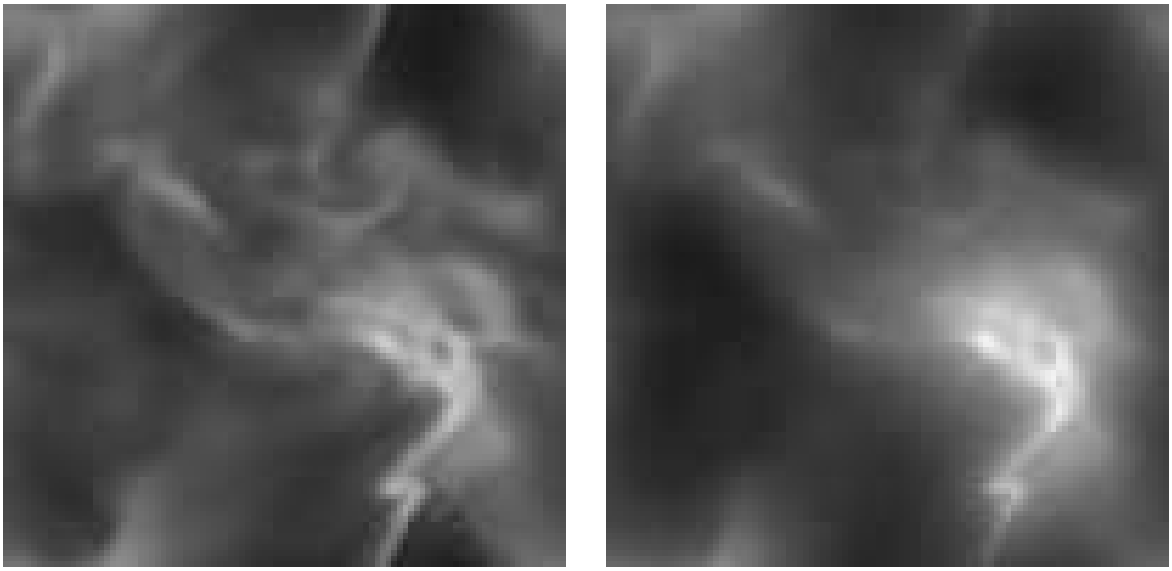

Fig. 3.— Two-dimensional cuts through the 3D density field in original form (*left panel*) and after modification to a spectral index of −5. Note that the modified-spectrum image appears smoother, because the relative importance of the small scales has been reduced in this case.

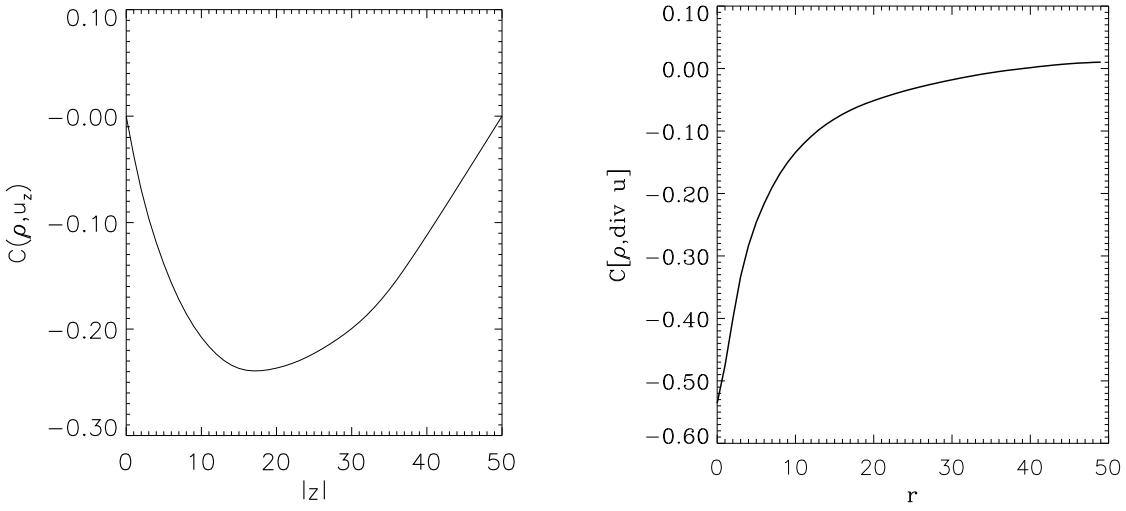

Fig. 4.— Cross-correlation between the density and the line-of-sight projection velocity fields (*a), left panel*), and between the density and the divergence of the total 3D velocity field (*b), right panel*). The density is significantly correlated with the velocity divergence, while the density-velocity correlation is weaker. The non-monotonous character of the correlation defines a range of scales at which the density-velocity correlation is maximal and the LP00 analysis requires testing.

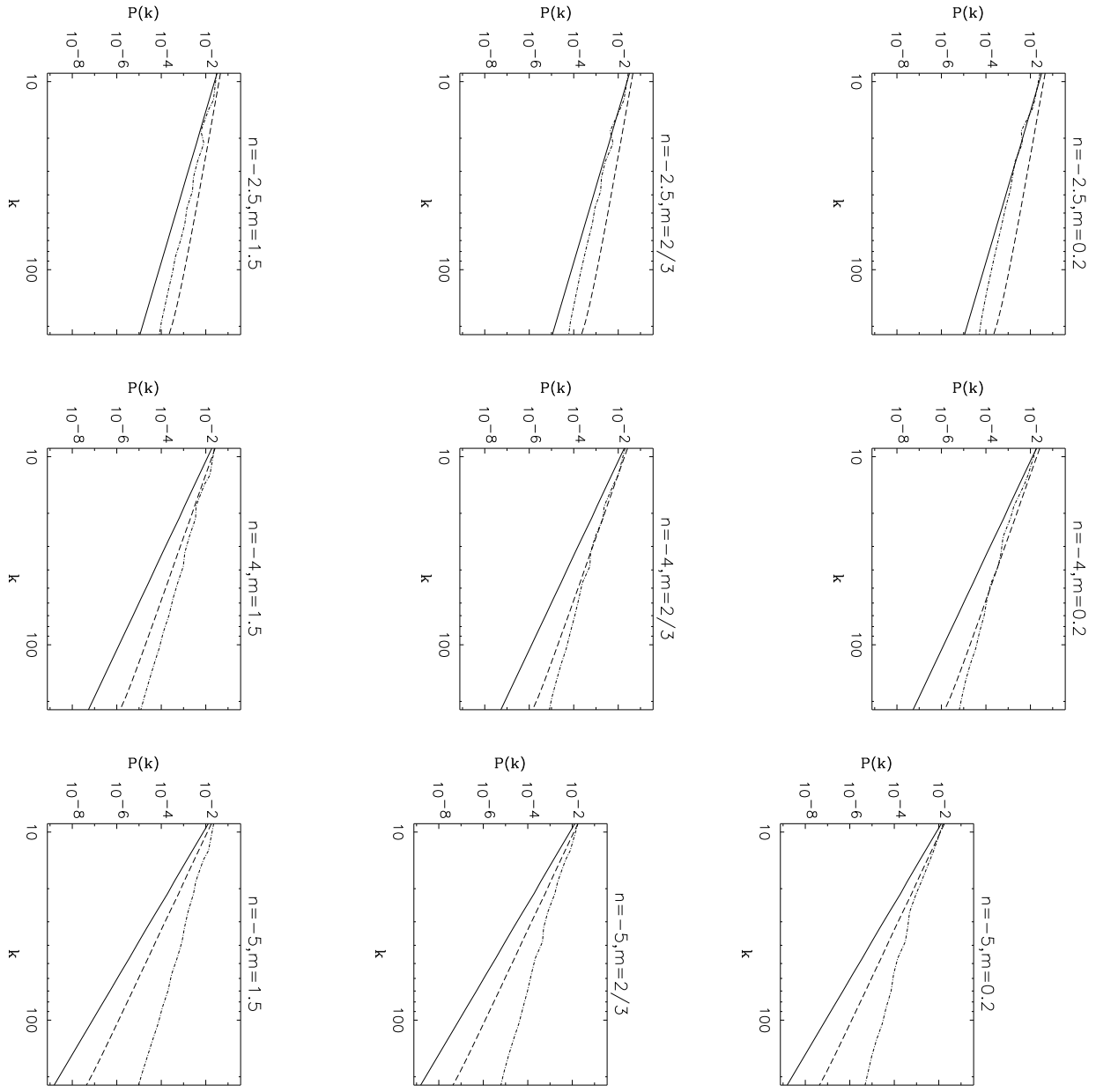

Fig. 5.— Spectra of the 3D density fields (*bold lines*) and of the emissivity in the 2D channel maps (*dash-dotted lines*) for all nine combinations of density and velocity spectral indices reported in Table 1. For comparison, the spectra of 2D *thin, spatial* slices of the density are also shown (*dashed lines*). The wavenumber k here is defined as $2\pi L/\lambda$, where L and λ are as in the caption to fig. 2.

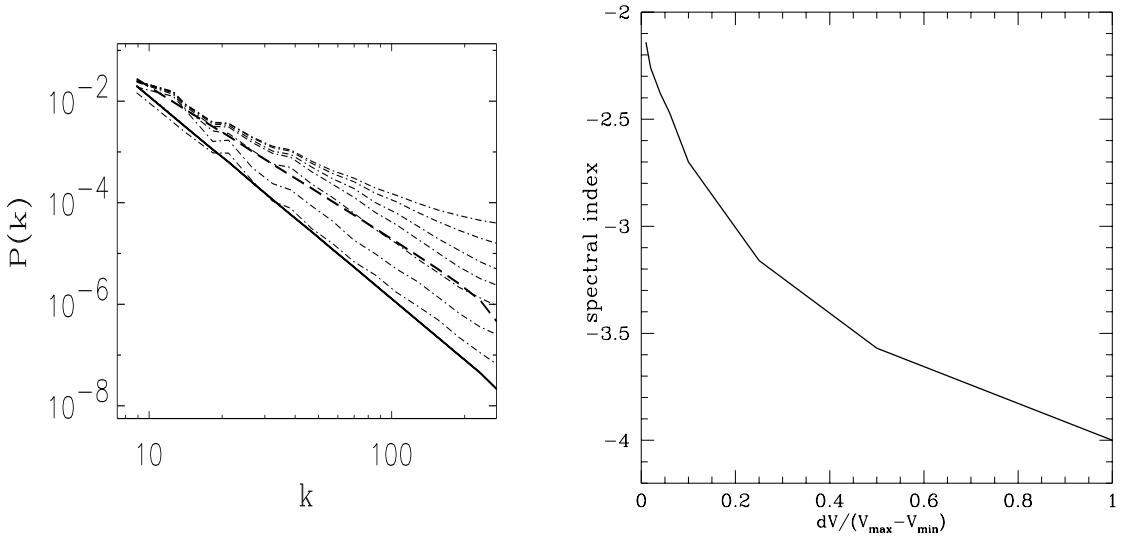

Fig. 6.— *Left Panel: Thin dash-dotted lines:* emissivity spectra for velocity slices of various widths, for velocity spectral index −4.5 and density index −4. From top to bottom, the curves correspond to slices of width 0.01, 0.02, 0.04, 0.06, 0.1 0.25, and 0.5 times ΔV. *Thick solid line:* power spectrum of the LOS-projected density field (i.e., column density). The emissivity spectra in the velocity slices are seen to approach the spectrum of column density as they get wider. *Thick dashed line:* power spectrum of a *thin* (1 grid cell) spatial density slice. The emissivity spectra in thin velocity slices are seen to be strongly influenced by the velocity field, as they have different slopes than the spectra of either the column density or the thin density spatial slice. *Right Panel:* Variation of the emissivity spectral index as a function of the velocity slice width for the same data cube.